

Detection of noise-corrupted sinusoidal signals with Josephson junctions

Giovanni Filatrella¹ and Vincenzo Pierro²

¹*CNR/SPIN and Dept. of Biological and Environmental Sciences,
University of Sannio, Via Port'Arsa, 11, I-82100 Benevento, IT*

²*Dept. of Engineering, University of Sannio,
Corso Garibaldi, 107, I-82100 Benevento, IT*

(Dated: November 20, 2018)

Abstract

We investigate the possibility of exploiting the speed and low noise features of Josephson junctions for detecting sinusoidal signals masked by Gaussian noise. We show that the escape time from the static locked state of a Josephson junction is very sensitive to a small periodic signal embedded in the noise, and therefore the analysis of the escape times can be employed to reveal the presence of the sinusoidal component. We propose and characterize two detection strategies: in the first the initial phase is supposedly unknown (incoherent strategy), while in the second the signal phase remains unknown but is fixed (coherent strategy). Our proposals are both suboptimal, with the linear filter being the optimal detection strategy, but they present some remarkable features, such as resonant activation, that make detection through Josephson junctions appealing in some special cases.

PACS numbers: 07.05.Kf, 85.25.Cp, 84.40.Ua, 05.10.Gg

I. INTRODUCTION

Detection of sinusoidal signals corrupted by Gaussian noise is, in principle, a completely solved problem. It can be proven that in the framework of statistical decision theory (Neyman-Pearson scheme) an adapted linear filter implemented via a Fourier transform is the optimal choice [1]. Unfortunately it is not always possible to apply such optimal detection strategy, due to a huge amount of data to process or to the extreme weakness of the signal to be detect. As an example we mention the all-sky all-frequency search for gravitational waves emitted by a pulsar [2], the search for continuous monochromatic signal in radio astronomy [3] and the detection of THz radiation [4]. When the optimal choice is not applicable, suboptimal strategies should be compared [5]: for example it has been proposed to use generic bistable systems [6, 7]. The general idea is the following: the oscillatory signal corrupted by noise is applied to a nonlinear bistable element that transforms the original signal to a new one, simpler to analyze. In other words, instead of applying a linear matched filter to the source signal, one inserts a nonlinear element; such insertion cannot improve the overall performance [8], but can make detection easier or can reduce the computational or memory burden.

Among nonlinear elements (like generic bistable devices [6] and superconducting systems [9]) a good candidate is the Josephson Junction [10] (henceforth JJ) for two important reasons: 1) JJs are extremely fast elements, that can easily operate above 100GHz and up to the THz region [11]; 2) JJs, being superconductive elements, can be cooled close to absolute zero or to the quantum noise limit [12], thus lessening the additional contribution of thermal noise from the bistable element. The detection of small signals in the presence of noise with JJs has been reported in two configurations: investigating the magnetic flux trapped by a JJ closed in a superconducting loop [13, 14] (thus forming a SQUID [10]) or analyzing the switching from the metastable locked solution to the running state of an underdamped isolated JJ [15]. The SQUID exhibits a standard double well potential equivalent to the classical case, well known in the context of stochastic resonance [16, 17] as a relevant phenomenon for signal detection [6, 18], although suboptimal [8]. However SQUIDS, even if they are very sensitive and well studied systems, meet a principal drawback in their limited bandwidth, typically bounded to few KHz [18, 19]. The escape from the static solution of single JJ [15], being extremely fast, seems to be promising for signal processing. In this paper we aim to characterize such a device as a detector.

The detection scheme that we propose is closely related to the general problem of passage over

a time-dependent barrier. More precisely, when the JJ passes the maximum of the time-dependent potential, switching from the static to the running solution, it sets the first passage time across an absorbing barrier [20]. So the mean time between the initial state and the switch (or absorption) can be interpreted as a mean first passage time. Signal detection is then based on the possibility of ascertaining if the first passage times are due to a constant barrier (no signal present) or by an oscillating barrier (signal is present).

II. MODEL AND DETECTION STRATEGIES

The tunnel of Cooper pairs and normal electrons through a JJ biased with a sinusoidal signal of amplitude S_0 , a noise signal $S(t)$ and an additive thermal noise $N(t)$ can be modeled by the Langevin equation [10]:

$$C \frac{d^2\varphi}{dt^2} + \frac{1}{R} \frac{d\varphi}{dt} + I_c \sin(\varphi) = I_B + S_0 \sin(\Omega t + \varphi_0) + S(t) + N(t). \quad (1)$$

Eq. (1) is called underdamped because of the presence of the second derivative, or non negligible capacitance. In normalized units the equation reads:

$$\ddot{\varphi} + \alpha \dot{\varphi} + \sin(\varphi) = \gamma + \varepsilon \sin(\omega \tilde{t} + \varphi_0) + \xi(\tilde{t}) + \eta(\tilde{t}). \quad (2)$$

Here $\alpha = (\hbar/2eI_c C)^{1/2}/R$ is the dissipation (I_c , R and C are the critical current, the resistance and the capacitance of the junction), $\gamma = I_B/I_c$, the dc bias due to the physical bias current I_B . These parameters can be adjusted in the experiments, although it is not easy to control dissipation (determined by the normal resistance R) one could in principle insert shunt resistors to achieve the desired level of dissipation. We have set $\alpha = 0.2$ and $\gamma = 0.6$ without performing any parameter optimization to devise the best compromise between signal detection performances and experimental simplicity: we have just fixed the parameters for numerical convenience. Furthermore $\varepsilon = S_0/I_c$ is the amplitude of the ac signal, $\omega_j = [2eI_c/(\hbar C)]^{1/2}$ the Josephson frequency, and $\tilde{t} = \omega_j t$ the normalized time. Overdot denote the derivative respect to \tilde{t} .

In Eq. (2) two random terms appear, η that represents thermal current fluctuations of intensity $\langle \eta(\tilde{t})\eta(\tilde{t}') \rangle = 2\alpha\theta\delta(\tilde{t}-\tilde{t}')$, ($\theta = 2ek_B T/(\hbar I_c)$ is the normalized temperature) and ξ that represents an additive noise with autocorrelation function of intensity D , viz $\langle \xi(\tilde{t})\xi(\tilde{t}') \rangle = 2D\delta(\tilde{t}-\tilde{t}')$, corrupting the external signal. To assume that the signal is only corrupted by an additive term is a simplification: noise can affect the signal in several ways, for instance as a bandpass noise,

multiplicative noise, phase noise, or as frequency fluctuations. We have focused on the simple case of additive noise (that is a paradigm in signal processing); however we expect that the results can be indicative of the behavior also for other noise sources. For instance frequency fluctuations of the drive in a JJ can be treated, in some limits, as an additive noise [21]. Quantum fluctuation contribute as an equivalent thermal source of temperature $\theta^* = e\omega_J/(\pi I_c)$ [14, 22], that can be confused with the stochastic effects [23]. Thus it is in principle always possible to decrease the temperature, proportional to θ , to reduce fluctuations to an unavoidable quantum noise level.

A washboard potential is associated with Eq. (2) [10, 24]:

$$U(\varphi) = -\gamma\varphi - \cos(\varphi). \quad (3)$$

The washboard potential (3) for $\gamma < 1$ gives rise to a barrier [24]:

$$\Delta U(\gamma) = 2[\sqrt{1 - \gamma^2} - \gamma \cos^{-1}(\gamma)]. \quad (4)$$

If the oscillating current is zero ($\varepsilon = 0$) for low noise ($\theta \ll D$, $D \ll \Delta U$) escape occurs at a rate r_0 [20]

$$r_0 \propto \tau_K^{-1} \exp\left(\frac{\Delta U}{D}\right). \quad (5)$$

Such a rate is related to the average escape time $\tau_0 = 1/r_0$ (τ_K is the Kramer prefactor, see [20]). The escape times can be directly measured in experiments [23, 25]. In fact when an underdamped junction leaves the metastable zero voltage state it switches to a running state with which is associated a voltage. It is therefore possible to measure the time elapsed from the application of the signal to the escape.

The possibility of experimentally determining the probability distribution of the escape times and the average escape rate is the key feature that we want to exploit for signal detection. More precisely, we propose to take advantage of the exponential dependence of the mean escape time upon the barrier height. The escape waiting time is highly sensitive to the amplitude of the signal [26] as noticed since the pioneering experiments [27] that reported the striking changes into the escape time distributions for the resonant activation of JJ. For the case of no signal, the expected residence time distribution is exponential, while for oscillating barriers the distribution is modified and the average changed. The phenomenon has been thoroughly analyzed for overdamped systems [28] with colored noise [30] and measured for underdamped systems [15]. For square wave signals, where a sudden switch of the barrier (4) between two values occurs, a remarkably

accurate estimate has been proposed [26]. Unfortunately, when a sinusoidal signal is embedded in noise and the barrier (4) is modulated, the formula of Ref. [26] is no longer valid. Moreover, the method used in Refs. [15, 26] assumes that the signal is applied with a known phase (φ_0 in Eq. (2)) and therefore the escape time distribution is a function of the initial phase [15]. In the context of signal detection, the frequency of the signal might be unknown, and therefore such approach could be inapplicable. In this paper we propose to use two procedures. The first can be implemented without knowledge of the phase (*incoherent detection*), and only relies on detection of the escape time and subsequent reset of the system to the bottom of the potential well (see Fig. 1). The second strategy (*coherent detection*) uses the phase parameter (that is supposed constant, although unknown) and hence is more similar to the approaches [15, 26].

The procedure that we propose for the incoherent detection strategy is the following: a) the signal-noise is applied with an unknown initial phase φ_0 in Eq. (2); b) when an escape occurs in the evolution of Eq. (2) (the junctions reaches the metastable state U_{max}) the time τ_i necessary for such an escape is recorded and the signal-noise is arrested or disconnected from the system; c) the JJ is reset to the bottom of the potential well U_{min} ; d) the signal-noise is reapplied, *i.e.* Eq. (2) is integrated adding $\omega\tau_i$ to the previous initial phase. We have numerically checked that after few iterations the memory of the initial phase φ_0 is lost and that the long term distribution of the escape times is independent of the choice of the initial phase. It is therefore also possible to apply the incoherent strategy if the initial phase is unknown.

In the second case (coherent detection strategy) one assumes that the frequency ω of the signal is fixed. Under such an hypothesis, we adopt the following procedure (for square signals it corresponds to the procedure of Ref. [15]): a) the signal-noise is applied with an unknown initial phase φ_0 to a JJ that is at rest in the bottom of the potential well (3). The phase between the signal and the JJ is therefore fixed, but concealed; b) when the escape occurs, the escape time τ_i to reach the metastable state U_{max} is recorded and the signal-noise is only arrested after a time that is a multiple of the period $2\pi/\omega$ of the external radiation to guarantee that the same (unknown) initial phase φ_0 of the signal is retrieved; c) the JJ is reset to the bottom of the potential well U_{min} to reproduce the same initial conditions as at point a); d) the signal is restarted, *i.e.* Eq. (2) is reapplied, and it will have with respect to the JJ the same initial phase φ_0 . We remark that the phase difference between the JJ and the signal, φ_0 , is frozen but unknown. To interpret the data it is necessary to reproduce the results for all values of φ_0 . In fact the distribution of the escape times depends upon the initial phase φ_0 , as will be discussed in Sect. IV.

We remark on the main difference between the two strategies: when the system switches from the locked to the running state in the incoherent strategy we immediately stop the application of the noise-signal, while in the coherent strategy we let the signal run to retrieve the initial phase.

For both strategies if the signal is digitally recorded, as it is the case for the all-sky-all-frequency search of gravitational waves emitted by a pulsar, a preliminary digital/analog conversion could be required to obtain a signal in the JJ frequency range. In this case it is possible to apply the recorded signal with a much faster time, in the GHz range or as fast as the electronics allows (while the real time signal might be slower) thus achieving a considerable speed up.

Typical Complementary Cumulative Distribution Function (CCDF) of the escape times in presence of a sinusoidal signal ($\varepsilon = 0.2$, broken lines) and without signal ($\varepsilon = 0$, solid line) have been simulated by numerical integration of Eq. (2) with the Euler method [29] and are shown in Fig. 2. Such a Figure can also be interpreted as the CCDF for the passage times of a particle in a well over an oscillating barrier (broken lines) or over a constant barrier (solid line).

From the data it is clear that the CCDF for the two strategies, coherent and incoherent, are very similar, with just a change in the slope and therefore a change in the average escape time.

III. RESULTS FOR INCOHERENT DETECTION

In Fig. 3 we show the estimated average escape times through U_{max} (see Fig. 1) vs ω of a phase particle subject to an external drive and detected with the incoherent strategy (dot-dashed line of Fig. 2). Around the normalized Josephson resonant frequency $\omega_0 = (1 - \gamma^2)^{1/4}$ the escape time is very sensitive to the external signal, in fact it exhibits a large dip, i.e. a pronounced deviation of the average escape time respect to the unperturbed value even for small ε/\sqrt{D} . (We recall that ε/\sqrt{D} is proportional to the signal to noise ratio, SNR). At low frequencies the deviations are less pronounced but still relevant, while for high frequencies one recovers the Kramer escape time of the unperturbed system [20]. It is clear that there is a wide range of frequencies $(0, \omega_0)$ where the analysis of the estimated average escape times $\langle \tau \rangle_S$ can give a clue to the presence of an external drive corrupted by noise, as they are different from the average of the escape times without the signal, τ_0 .

To make such analysis more quantitative, in Fig. 4 we have adopted the Kumar-Carroll (K-C) index d_{KC} [31]:

$$d_{KC} = \frac{|\langle \tau \rangle_S - \langle \tau \rangle_N|}{\sqrt{\frac{1}{2}(\sigma^2(\tau)_S + \sigma^2(\tau)_N)}}, \quad (6)$$

where $\langle \tau \rangle_S, \langle \tau \rangle_N$ are the estimated average escape time over a prescribed interval T , with and without signal, respectively. We have also denoted with $\sigma(\tau)_S, \sigma(\tau)_N$ the corresponding estimated standard deviations. The K-C index (6) is related to the receiving operating characteristics (ROC) of the detector, and as a rule of thumb is well approximated by the ROC of a matched filter with signal to noise ratio equal to d_{KC} [31]. In Fig. 4 it is evident, as expected, that d_{KC} grows by increasing the observation time T . The statistical analysis of Fig. 4 confirms the result of Fig. 3, *i.e.* the existence of a peak at the geometric resonance ω_0 ($d_{KC} \simeq 25$ at $T \simeq 10^4(2\pi/\omega_0)$), and of an interesting region for lower frequencies ($d_{KC} \simeq 5$), while the method seems inapplicable at frequencies above ω_0 ($d_{KC} \simeq 1$). From Figs. 3 and 4 it is also clear that there is no evidence of stochastic resonance [17] due to resonant activation, or prominent signal detection at matching between the external drive frequency and the noise induced unperturbed escape rate, as reported for instance in Ref.[15]. In contrast to stochastic resonance the results of Figs. 3 and 4 only display a noise independent resonance at ω_0 . This difference can be ascribed to the peculiar manner in which the external signal is applied. In the incoherent strategy the system loses memory of the phase of the signal at the passage through the absorbing barrier (see Sect. II). Instead in Ref.[15] the system is reset after each switch – such reset corresponds to the coherent detection to be analyzed in Sect. IV.

In Fig. 5 we show the K-C index for several values of the ratio ε/\sqrt{D} . The purpose is to emphasize the behavior for small SNR, when reliable stochastic simulations are prohibitive. The data reduction demonstrates that the K-C index decreases roughly as an inverse power law of the SNR; the best fit procedure gives an upper bound of ≈ 1.5 for the exponent. Extrapolating the results, it is thus possible to infer the behavior for SNR's lower than those reported in the figure. We recall that these performances refer to a specific signal duration $T = 2 \cdot 10^5 (2\pi/\omega_0)$ in Fig.5. The K-C index increases extending the detection time T , insofar as the K-C index is roughly proportional to \sqrt{T} , see also Fig. 4. Thus combining the numerical power estimated by Fig. 5 and the square root dependence of the K-C index captured by the data of Fig. 4 it is possible to predict that to keep a fixed d_{KC} while lowering ε/\sqrt{D} , the detection interval should increase as $T \approx (\varepsilon/\sqrt{D})^{-3}$. Consequently, by extending the detection time T one can also achieve the desired level of the K-C index for low values of SNR. As expected, the matched filter requires

shorter detection time ($T \approx (\varepsilon/\sqrt{D})^{-2}$).

IV. RESULTS FOR COHERENT DETECTION

In Section II we discussed the possibility of detecting a signal at a predetermined frequency ω employing a coherent detection strategy. In such strategy the signal is always applied with the same initial phase. The analysis of the estimated average escape time in presence of a signal with initial phase $\varphi_0 = 0$ is reported in Fig. 6. The data show a remarkable dip at low frequency ($\omega \simeq 0.01$), that is not present in the incoherent detection strategy, see Fig. 3. To compare the performances we analyze the K-C index (6) in Fig. 7. This analysis, as does the simpler analysis of Fig. 6, confirms the existence of an interesting region ($d_{KC} \simeq 10$) at low frequency ($\omega \simeq 0.01$) that is not present in the incoherent strategy (see Fig.4).

In Fig. 8 we show the dependence of the K-C index as a function of the signal scaled amplitude ε/\sqrt{D} (compare to Fig. 5 for the incoherent analysis). This analysis leads to the same conclusion as for the incoherent strategy, *i.e.* by increasing the detection time $T \approx (\varepsilon/\sqrt{D})^{-3}$ one can achieve the desired level of the K-C index.

A second resonant condition for the coherent detection strategy occurs at the angular frequency:

$$\omega = C(\varphi_0) \left(\frac{2\pi}{\tau_0} \right), \quad (7)$$

where τ_0 is the escape time of Eq. (2) for $\varepsilon = 0$. The factor $C(\varphi_0)$ reads 1/4 for $\varphi_0 = 0$ and is different from the frequency condition of the standard stochastic resonance [7]. This difference has been also reported in the experimental findings of Ref. [15, 26]. In Fig. 9 the frequency relation (7) is further elucidated: we show for different values of D the estimated escape time. From the figure it is clear that the largest deviation of the signal induced average escape time $\langle \tau \rangle_S$ occurs at the matching condition described by Eq. (7) over a wide range of noise intensity, $0.04 \leq D \leq 0.2$. Fig. 9 thus indicates the presence of a stochastic resonance between the noise (which determines τ_0) and the frequency ω of the external signal. We ascribe the change in Eq. (7) with respect to the traditional stochastic resonance to the peculiar choice of initial conditions. The reset of the initial conditions changes the effective waveform of the signal, see Fig. 10. Let us define $P(\varphi_0)$ as the time from the initial phase and the phase that corresponds to the maximum of the signal and therefore to the minimum of the barrier (4). Assuming that the effective waveform of the signal is of the type depicted in Fig. 10, the matching condition for stochastic resonance shown in Fig.

11 is that the barrier reaches a minimum in a time $P(\varphi_0)$ close to the noise induced escape from the lowest energy well. Such resonant condition depends upon the initial phase φ_0 ; in Fig. 12 we report the scaled deviations of the average estimated escape time in presence of the signal as a function of the ratio $2\pi/\tau_0\omega$ for different values of the initial phase φ_0 . We hypothesize that the horizontal axis positions of the relative minimal $C(\varphi_0)^{-1}$ in Fig. 12a correspond to the resonant condition of Fig.11. In other words, we observe that a resonant condition occurs when the time $\tau_0(\Delta U_-)$ to escape the minimum barrier (denoted by ΔU_- in Fig.11) matches the time in which the oscillating barrier reaches a minimum:

$$\tau_0(\Delta U_-) = P(\varphi_0). \quad (8)$$

The resonance phenomenon described by Eq. (8) is evident in Fig.12a where the barrier reaches a minimum in a single ramp-up. Eq. (8) has been compared with numerical data in Fig. 13 and shows excellent agreement. This simple picture does not hold when the barrier non-monotonically reaches the minimum; in fact in Fig.12b the condition (8) is not valid for $\varphi_0 = \pi$.

We wish to underline the following remarks about Eq. (8):

- 1) The prediction of Eq. (8) in the case $\varphi_0 = 0$, $P(\varphi_0) = (1/4)(2\pi/\omega_0)$, correctly describes the experimental finding of an harmonically driven underdamped JJ , see Ref. [26];
- 2) When the barrier decreases monotonically ($-\pi/2 \leq \varphi_0 \leq \pi/2$) and the escape occurs in a single ramp-up of the signal (see Fig. 10), the physical situation is similar to a fluctuating barrier [26, 32–34]: the time in which the washboard potential reaches the minimum, $P(\varphi_0)$ in our notation, plays the role of the barrier flipping rate in Refs. [26, 32–34].
- 3) By varying the bias current γ (which is an external parameter) one can set the most appropriate barrier (see Eq.s (4) and (5)) to match the resonant condition (8).

A qualitative argument to understand the behavior when the signal does not reach a maximum in a single ramp-up (see Fig.12b) can be sketched following Ref. [33], where it has been noticed that a resonant activation occurs in two cases:

- a) The low and high frequency limits of the escape times are identical: an extremum occurs if the derivative with respect to ω of the barrier is nonzero;
- b) The low and high frequency limits of the escape times are different: an extremum occurs if the derivative with respect to ω of the escape time is opposite to the difference of the limits.

The low frequency limit of the escape time can be estimated with an heuristic argument (see the Appendix for details):

$$\tau(\varphi_0, \omega) \approx \tau_K e^{-\frac{\Delta U(\varepsilon \sin(\varphi_0) + \gamma)}{D}} (1 + A\omega\varepsilon \cos(\varphi_0)) + O((\omega\tau(\varphi_0, \omega))^2), \quad (9)$$

where τ_K is the Kramer prefactor and the positive constant A reads:

$$A = -\frac{\tau_K}{D} e^{-\frac{\Delta U(\varepsilon \sin(\varphi_0) + \gamma)}{D}} \Delta U'(\varepsilon \sin(\varphi_0) + \gamma). \quad (10)$$

The high frequency limit (see the Appendix) is given by the time independent potential:

$$\tau(\varphi_0, \omega) \approx \tau_K \exp \left[-\frac{\Delta U(\gamma)}{D} \right] + O \left(\frac{1}{\omega\tau(\varphi_0, \omega)} \right). \quad (11)$$

A consequence of Eqs. (9) and (11) is that for $0 \leq \varphi \leq \pi$ the low frequency limit of the barrier is lower than the high frequency limit, and therefore the escape time will be longer (the reverse situation will be observed in the range $-\pi \leq \varphi \leq 0$). From Eq. (9) we are able to compute the following derivative

$$\frac{d\tau(\varphi_0, \omega)}{d\omega} \approx \tau_K e^{-\frac{\Delta U(\varepsilon \sin(\varphi_0) + \gamma)}{D}} A\varepsilon \cos(\varphi_0) + O(\omega\tau(\varphi_0, \omega)). \quad (12)$$

Eq. (12), valid in the low ω regime, shows that the corrections to the zero frequency limit $\tau(\varphi_0, 0) \approx \tau_K e^{-\frac{\Delta U(\varepsilon \sin(\varphi_0) + \gamma)}{D}}$ have the same sign of the derivative of the external drive, i.e. $\text{sign}(\cos \varphi_0)$. The results of Fig.12 confirm this picture: a resonance, or a non monotonic behavior is observed for all initial phases but $\varphi_0 = \pm\pi/2$ (where the signal derivative vanishes and one should consider higher order corrections) and is most evident for $\varphi_0 = 0, \pi$ - where the signal derivative is at a maximum -. In the most effective cases , $\varphi_0 = 0$ and $\varphi_0 = \pi$, the former leads to the condition (8) with $C(\varphi_0)$ correctly predicted by Eq. (7) (see also Fig.13), while the latter ($\varphi_0 = \pi$) exhibits a different frequency relation when the signal maximum not reached in a single ramp-up.

V. CONCLUSIONS

We employed the escape times of a JJ from the locked state as a statistic tool to detect sinusoidal signals corrupted by noise. We have determined the main features of such a statistical detector for both incoherent and coherent detection. For the former we found that the detector: *i*) is most sensitive to the signal in proximity to the junction resonance, *ii*) shows a clearly asymmetric

behavior in frequency: very low sensitivity above the resonance, and relatively good performance for lower frequencies. In the coherent case, which requires *a priori* knowledge of the applied frequency, the performance depends upon the initial phase. For an appropriate choice of the initial phase it is also evident a resonant activation, *i.e.* a matching condition between the noise induced escape time and the external frequency, Eq. (8), well fits the numerical data. Our analysis of the role of the initial phase extends the previously observed resonant escape [26]. Future research could be directed towards: *i*) development of better detection strategies; *ii*) coupling two or more elements to exploit the properties of arrays of JJs [35]; and *iii*) a more accurate analytical treatment of phase dependent resonant activation phenomenon.

We remark that the detection scheme based on JJs is suboptimal, but could prove fast and capable of operation at very low temperatures, with low intrinsic noise. It is therefore in niche applications where speed and reduced noise are essential that this approach could be considered. Finally, a few words of caution: while we have analyzed the physical principles underlying JJs as possible detectors, practical applications require a deeper analysis of circuit design and of technological limitations.

We wish to thank S. Pagano and I. M. Pinto for fruitful discussions and R. Newrock for a critical reading of the manuscript.

Appendix

In this Appendix we give the asymptotic behavior of $\tau(\varphi_0, \omega)$ in the slow and fast frequency limit ($\omega \rightarrow 0$ and $\omega \rightarrow \infty$). To compute the slow frequency behavior of the average escape time we use, following Ref. [17], periodically modulated escape rates of Arrhenius type. In this connection we have:

$$\tau(\varphi_0, \omega) \approx \langle \tau_K \exp[-\frac{\Delta U(\tilde{\gamma}(\tilde{t}))}{D}] \rangle \quad (A1)$$

where $\tilde{\gamma}(\tilde{t}) = \gamma + \varepsilon \sin(\omega\tilde{t} + \varphi_0)$ is the time dependent bias and τ_K is the Kramer escape rate prefactor. Since we are interested in computing the asymptotic limit $\omega \rightarrow 0$, there exists a frequency such that $\omega\tilde{t} \ll \omega 4\langle\tau\rangle \ll 1$, where, due the exponential like tail of the escape time distribution, the probability of occurrence of an escape time greater than $4\langle\tau\rangle$ is negligible. Accordingly, we expand the average escape time in Taylor series in the variable $\omega\tilde{t}$ and due to the exponential like distribution we approximation have the estimates $\langle\tilde{t}\rangle \approx \tau(\varphi_0, \omega)$, $\langle\tilde{t}^2\rangle \approx 2\tau(\varphi_0, \omega)^2$. The Taylor expansion of Eq. (A1) reads:

$$\tau(\varphi_0, \omega) \approx \tau_K e^{-\frac{\Delta U(\varepsilon \sin(\varphi_0) + \gamma)}{D}} \left(1 - \frac{\varepsilon\omega}{D} \tau(\varphi_0, \omega) \cos(\varphi_0) \Delta U'(\varepsilon \sin(\varphi_0) + \gamma) \right) + O((\omega\tau(\varphi_0, \omega))^2). \quad (A2)$$

In the previous equation $\tau(\varphi_0, \omega)$ appear on the right side of the formula (A2), it can be consistently eliminated by an iterative substitution (and truncation) of (A2) in itself. By defining the parameter :

$$A = -\frac{\tau_K}{D} e^{-\frac{\Delta U(\varepsilon \sin(\varphi_0) + \gamma)}{D}} \Delta U'(\varepsilon \sin(\varphi_0) + \gamma) \quad (A3)$$

Eq. (A2) can therefore be written:

$$\tau(\varphi_0, \omega) \approx \tau_K e^{-\frac{\Delta U(\varepsilon \sin(\varphi_0) + \gamma)}{D}} (1 + A\omega\varepsilon \cos(\varphi_0)) + O((\omega\tau(\varphi_0, \omega))^2). \quad (A4)$$

By using (4), the condition $A > 0$ holds.

The asymptotic limit $\omega \rightarrow \infty$ is obtained by noting that fast oscillation can not be followed by the system dynamic [20]. We have:

$$\tau(\varphi_0, \omega) \approx \tau_K \exp \left[-\frac{\Delta U(\gamma)}{D} \right] + O \left(\frac{1}{\omega\tau(\varphi_0, \omega)} \right). \quad (A5)$$

-
- [1] C.W. Helstrom, *Statistical Theory of Detection* (Pergamon, New York, 1968).
- [2] P. Jaranowski, A. Krolak, and B.F. Schutz, *Phys. Rev. D* **58**, 063001 (1998).
- [3] C.J. Salter, D.T. Emerson, H. Steppe, and C. Thum, *Astronomy and Astrophysics* **225**, 167 (1989),
- [4] M.D. Mittleman *Sensing with Terahertz Radiation* (Springer, Berlin, 2003).
- [5] B. Krishnan, A.M. Sintes, M.A. Papa, B.F. Schutz, S. Frasca, and C. Palomba, *Phys. Rev. D* **70**, 082001 (2004).
- [6] M.E. Inchiosa and A.R. Bulsara, *Phys. Rev. E* **53**, R2021 (1996).
- [7] L. Gammaitoni, P. Hänggi, P. Jung, and F. Marchesoni, *Rev. Mod. Phys.* **70**, 223 (1998).
- [8] V. Galdi, V. Pierro, and I.M. Pinto, *Phys. Rev. E* **57**, 6470 (1998).
- [9] A.V. Khudchenko, V.P. Koshelets, P.N. Dmitriev, A. B. Ermakov, P.A. Yagoubov, and O.M. Pylypenko, *Supercond. Sci. Technol.* **22**, 085012 (2009).
- [10] A. Barone and G. Paternò, *Physics and Application of Josephson Effect* (John Wiley, New York, 1982)
- [11] L. Ozyuzer, A.E. Koshelev, C. Kurter, N. Gopalsami, Q. Li, M. Tachiki, K. Kadowaki, T. Yamamoto, H. Minami, H. Yamaguchi, T. Tachiki, K.E. Gray, K.W. Kwok, and U. Welp, *Science* **318**, 1291 (2007).
- [12] F. Chiarello, C. Cosmelli, A. Costantini, G. Diambri-Palazzi, P. Carelli, R. Cristiano, and L. Frunzio, *J. Appl. Phys.* **80**, 2922 (1996).
- [13] A.M. Glukhov, A.G. Sivakov, and A.V. Ustinov, *Low Temp. Phys.* **28**, 383 (2002).
- [14] N. Grønbech-Jensen, M.G. Castellano, F. Chiarello, M. Cirillo, C. Cosmelli, L.V. Filippenko, R. Russo, and G. Torrioli, *Phys. Rev. Lett.* **93**, 107002 (2004).
- [15] G. Sun, N. Dong, G. Mao, J. Chen, W. Xu, Z. Ji, L. Kang, P. Wu, Y. Yu, and D. Xing, *Phys. Rev. E* **75**, 021107 (2007).
- [16] L. Gammaitoni, F. Marchesoni, E. Menichella-Saetta, and S. Santucci, *Phys. Rev. Lett.* **62**, 349 (1989).
- [17] B. McNamara and K. Wiesenfeld, *Phys. Rev. A* **39**, 4854 (1989).
- [18] R. Rouse, S. Han, and J.E. Lukens, *Appl. Phys. Lett.* **66**, 108 (1995).
- [19] A.D. Hibbs, A.L. Singsaas, E.W. Jacobs, A.R. Bulsara, J.J. Bekkedahl, and F. Moss, *J. App. Phys.* **77**, 2582 (1995).
- [20] H. Risken, *The Fokker-Planck Equation: Methods of Solution and Applications* (Springer, Berlin, 1989)

- [21] G. Filatrella, B.A. Malomed, and S. Pagano, Phys. Rev. E **65**, 051116 (2002).
- [22] I. Affleck, Phys. Rev. Lett. **46**, 388 (1981).
- [23] M.H. Devoret, J.M. Martinis, and J. Clarke, Phys. Rev. Lett. **55**, 1908 (1985).
- [24] E. Ben-Jacob and D.J. Bergman, Phys. Rev. A **29**, 2021 (1984).
- [25] Y. Yu, Y. Zhang, W. Qiu, S. Li, S. Han, and Z. Wang, Superc. Sci. Technol. **15**, 555 (2002).
- [26] Y. Yu and S. Han, Phys. Rev. Lett. **91**, 127003 (2003).
- [27] M.H. Devoret, D. Esteve, J.M. Martinis, A. Cleland, and J. Clarke, Phys. Rev. B **36**, 58 (1987).
- [28] N. Berglund and B. Guentz, Europhys. Lett. **70**, 1 (2005).
- [29] R. Mannella, in *Stochastic Processes in Physics, Chemistry and Biology*, J.A. Freund and T. Pöschel eds., p. 353 (Springer, Berlin, 2001).
- [30] G. Augello, D. Valenti, A.L. Pankratov, and B. Spagnolo, Eur. Phys. J. B **70**, 145 (2009).
- [31] B.V.K.V. Kumar and C.W. Carroll, Opt. Eng. **23**, 732 (1984).
- [32] M. Boguñá, J.M. Porrà, J. Masoliver, and K. Lindenberg, Phys. Rev. E **57**, 3990 (1998).
- [33] J.M. Porrà, Phys. Rev. E **55**, 6533 (1997).
- [34] C.R. Doering and J.C. Gadoua, Phys. Rev. Lett. **69**, 2318 (1992).
- [35] R.S. Newrock, C.J. Lobb, U. Geigenmuller, and M. Octavio, Solid State Physics **54**, 263 (1999).

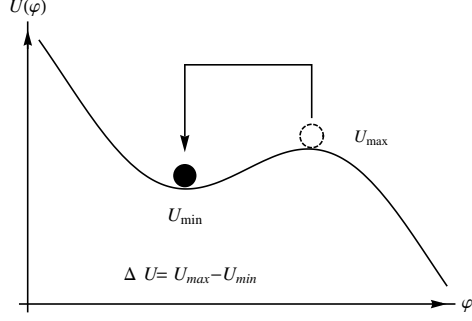


FIG. 1: A picture of the potential barrier and of the detection procedure. When the phase (depicted as a dashed circle in figure) reaches the top of the barrier from the left, the system is restarted with a suitable initial phase from the bottom (black disk in figure) of the potential well $U(\varphi)$.

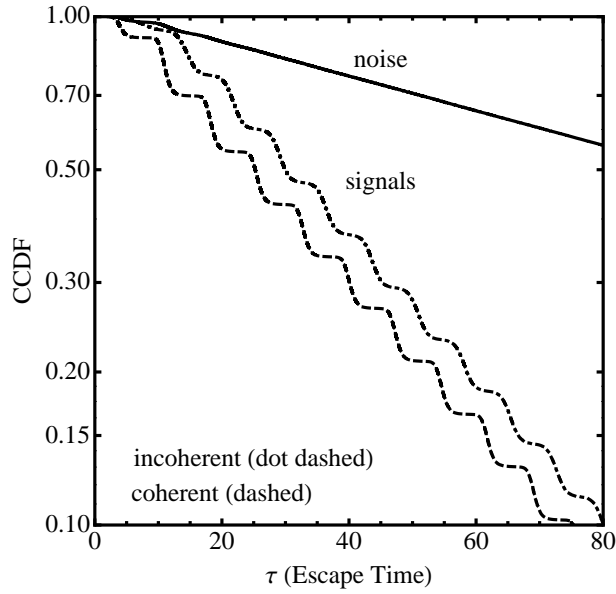


FIG. 2: The Complementary Cumulative Distribution Function (CCDF) of the escape time with signal $\varepsilon = 0.2$ in the incoherent (dot-dashed line) or coherent (dashed line) case. We also show the response to pure noise (solid line). The initial phase for the coherent strategy is $\varphi_0 = 0$. Parameters are: $\gamma = 0.5$, $\alpha = 0.2$, $\omega = 0.86$, $D = 0.05$, $\omega_0 = (1 - \gamma^2)^{1/4} \simeq 0.93$

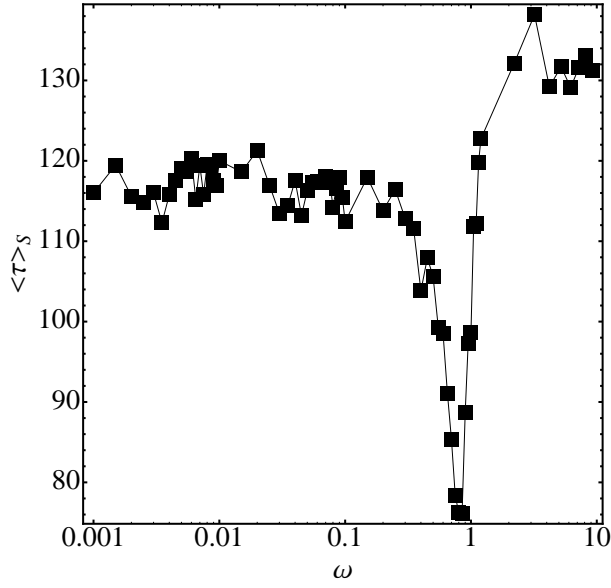


FIG. 3: Typical estimated $\langle \tau \rangle_S$ as a function of ω ($T = 2 \cdot 10^5 \cdot 2\pi/\omega_0$) for the incoherent detection strategy. Parameters are: $\gamma = 0.5$, $\alpha = 0.2$, $D = 0.05$, $\varepsilon = 0.1$. The average escape time in absence of the signal is $\tau_0 = 134.6$.

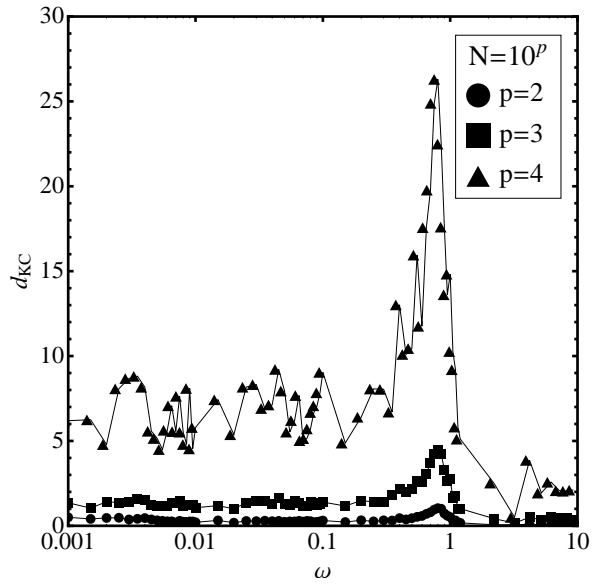


FIG. 4: The dependence of the K-C index as a function of angular frequency for parameters $\gamma = 0.5$, $\alpha = 0.2$, $D = 0.05$, $\varepsilon = 0.1$ in the case of the incoherent detection strategy. The curves displayed are for different observation time $T = 2\pi N/\omega_0$, where $N = 10^p$.

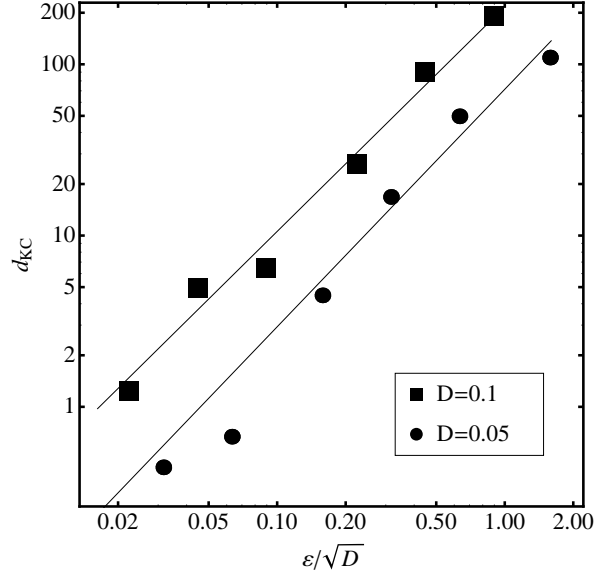


FIG. 5: The dependence of K-C index as a function of scaled signal amplitude ε/\sqrt{D} (proportional to the SNR) for the incoherent detection strategy. The parameters used are $\gamma = 0.5$, $\alpha = 0.2$, $\omega = \omega_0$, $T = 2 \cdot 10^5 \cdot 2\pi/\omega_0$.

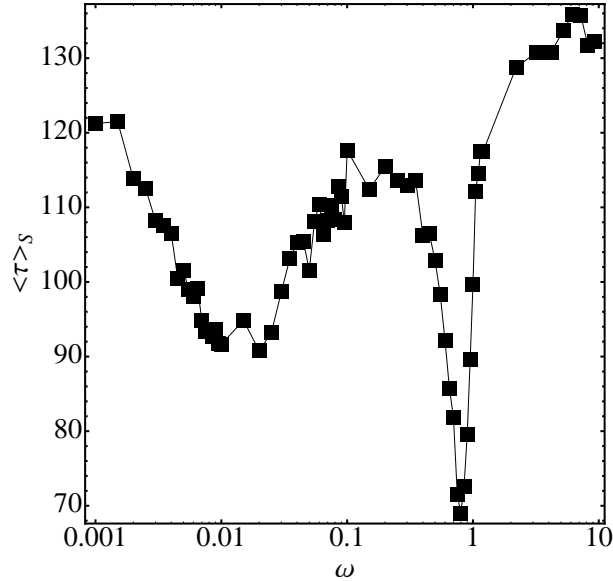


FIG. 6: Typical estimated $\langle \tau \rangle_S$ as a function of ω ($T = 2 \cdot 10^5 \cdot 2\pi/\omega_0$) for the coherent detection strategy. Parameters are $\gamma = 0.5$, $\alpha = 0.2$, $D = 0.05$, $\varepsilon = 0.1$, $\varphi_0 = 0$. The average escape time in absence of the signal is $\tau_0 = 134.6$.

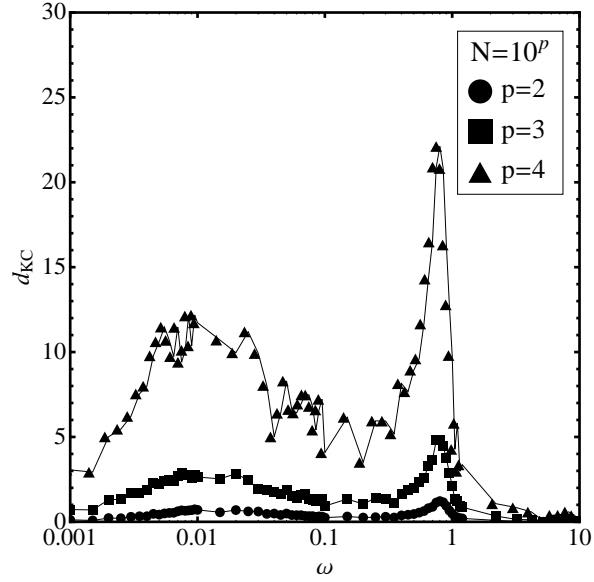


FIG. 7: The dependence of K-C index as a function of scaled angular velocity for the coherent detection strategy. Parameters are $\gamma = 0.5$, $\alpha = 0.2$, $D = 0.05$, $\varepsilon = 0.1$, $\varphi_0 = 0$. The curves displayed are for different observation time $T = 2\pi N/\omega_0$, where $N = 10^p$.

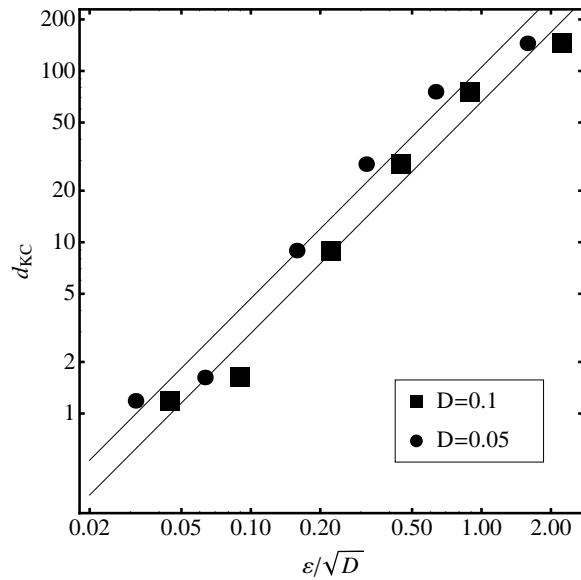


FIG. 8: The dependence of K-C index as a function of scaled signal amplitude ε/\sqrt{D} (proportional to the SNR) for the coherent detection strategy. The parameters used are $\gamma = 0.5$, $\alpha = 0.2$, $\omega = \omega_0$, $T = 2 \cdot 10^5 \cdot 2\pi/\omega_0$.

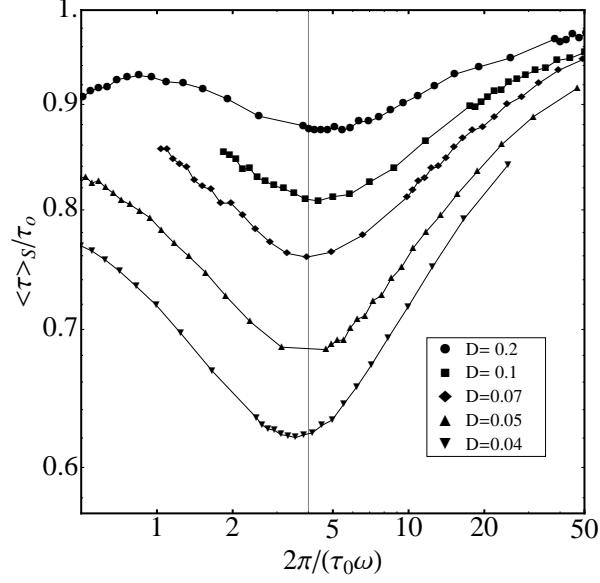


FIG. 9: Scaled estimated average escape time $\langle \tau \rangle_S$ in presence of signal, vs scaled period $2\pi/\tau_0\omega$ for different values of D in the case of coherent strategy (initial phase $\varphi_0 = 0$). The parameters used are $\gamma = 0.5$, $\alpha = 0.2$, $\varepsilon = 0.1$, τ_0 is the $\varepsilon = 0$ escape time. The vertical grid line indicates the resonant condition (7).

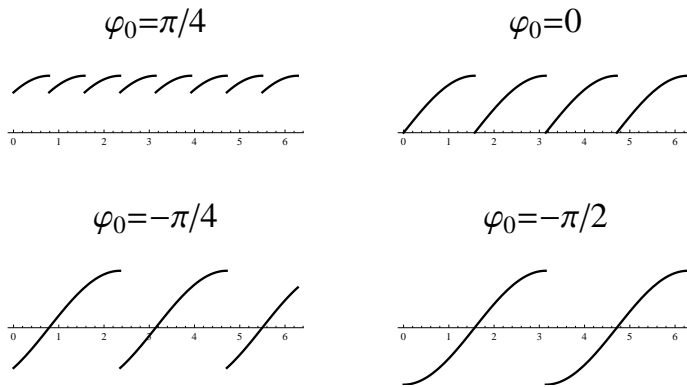


FIG. 10: Effective waveforms for a system prepared with initial phase $\varphi_0 = -\pi/2, -\pi/4, 0, \pi/4$. The figures show the sinusoidal drive between the initial phase φ_0 and the maximum of the signal, $\varphi = \pi/2$.

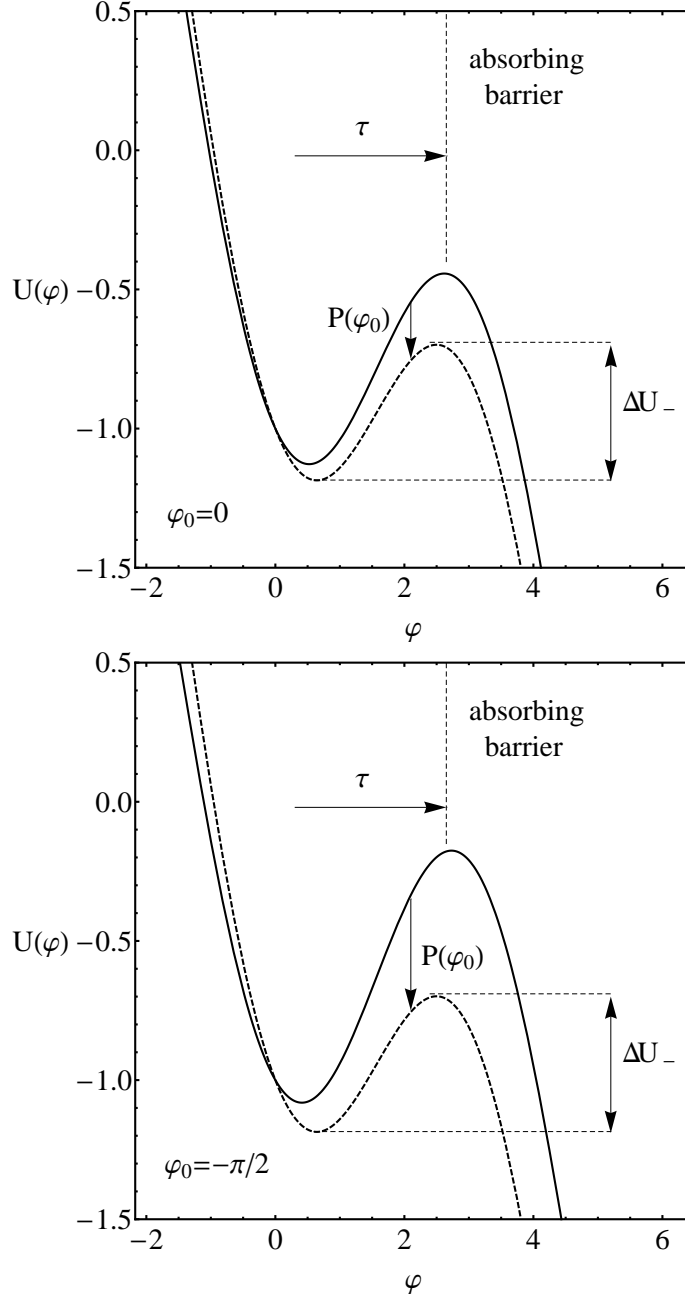


FIG. 11: The figures show the JJ potential $U(\varphi) = -\bar{\gamma}\varphi - \cos(\varphi)$ as a function of the phase. We consider $\bar{\gamma} = \gamma + \varepsilon \cos(\varphi_0)$ with initial phase $\varphi_0 = 0$ (top) or $\varphi_0 = -\pi/2$ (bottom); for illustrative purpose $\gamma = 0.5$ and $\varepsilon = 0.1$. The time $P(\varphi_0)$ is defined as the time between the application of the signal (with initial phase $\varphi_0 = 0, -\pi/2$) and the lowest height of the barrier, ΔU_- . The first passage time τ is defined as the time to overcome the maximum of the barrier (the vertical dashed line). The resonance defined by Eq. (8) states that a minimum of the passage time occurs when are equal the time in which the external signal reduces the barrier to the lowest value and the escape time from such barrier, assumed to be static.

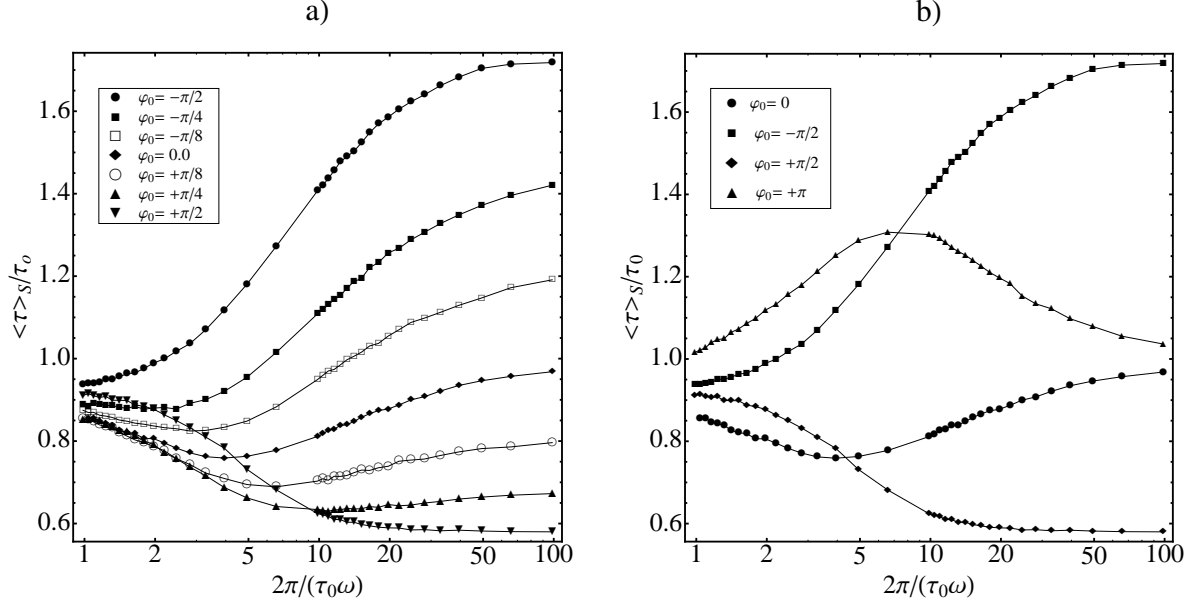


FIG. 12: The dependence of the average escape time $\langle \tau \rangle_S$ (scaled to τ_0) for the coherent detection strategy as a function of signal scaled period $2\pi/\omega$ for different values of the initial phase φ_0 . In panel a) we show the escape times when the effective waveform is monotonic, *i.e.* $-\pi/2 \leq \varphi_0 \leq \pi/2$; in panel b) we show the four limit cases $\varphi_0 = 0, \pi/2, \pi, -\pi/2$. We underline that for $\varphi_0 = \pi$ the non monotonic behavior of the effective waveform (the maximum is not reach in a single ramp-up) leads to a maximum in the escape time. The parameters used are $\gamma = 0.5, \alpha = 0.2, \varepsilon = 0.1, D = 0.07$.

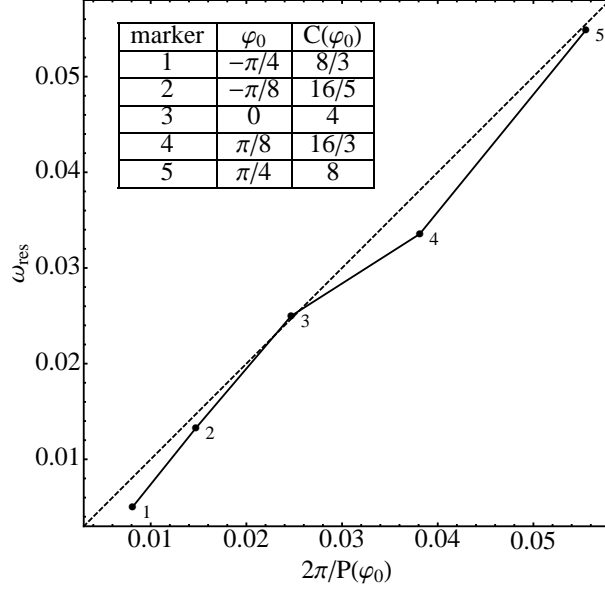


FIG. 13: The dependence of the resonant frequency as a function of $2\pi/P(\varphi_0)$, proportional to the inverse time between the initial phase and the maximum of the signal, see Fig. 11. The dashed line corresponds to the prediction of Eq. (8). Parameters are $\gamma = 0.5$, $\alpha = 0.2$, $\varepsilon = 0.1$, $D = 0.07$.